

# Generating Contrastive Explanations with Monotonic Attribute Functions

Ronny Luss<sup>1\*</sup>, Pin-Yu Chen<sup>1</sup>, Amit Dhurandhar<sup>1</sup>, Prasanna Sattigeri<sup>1</sup>  
Yunfeng Zhang<sup>1</sup>, Karthikeyan Shanmugam<sup>1</sup>, and Chun-Chen Tu<sup>2</sup>

February 3, 2022

## Abstract

Explaining decisions of deep neural networks is a hot research topic with applications in medical imaging, video surveillance, and self driving cars. Many methods have been proposed in literature to explain these decisions by identifying relevance of different pixels, limiting the types of explanations possible. In this paper, we propose a method that can generate contrastive explanations for such data where we not only highlight aspects that are in themselves sufficient to justify the classification by the deep model, but also new aspects which if added will change the classification. In order to move beyond the limitations of previous explanations, our key contribution is how we define "addition" for such rich data in a formal yet humanly interpretable way that leads to meaningful results. This was one of the open questions laid out in [6], which proposed a general framework for creating (local) contrastive explanations for deep models, but is limited to simple use cases such as black/white images. We showcase the efficacy of our approach on three diverse image data sets (faces, skin lesions, and fashion apparel) in creating intuitive explanations that are also quantitatively superior compared with other state-of-the-art interpretability methods. A thorough user study with 200 individuals asks how well the various methods are understood by humans and demonstrates which aspects of contrastive explanations are most desirable.

## 1 Introduction

With the explosion of deep learning [8] and its huge impact on domains such as computer vision and speech, amongst others, many of these technologies are being implemented in systems that affect our daily lives. In many cases, a negative side effect of deploying these technologies has been their lack of transparency [25], which has raised concerns not just at an individual level [32] but also at an organization or government level.

---

\*First five authors have equal contribution. 1 and 2 indicate affiliations to IBM Research and University of Michigan respectively.

There have been many methods proposed in literature [1, 14, 19, 23, 29] that explain predictions of deep neural networks based on the relevance of different features or pixels/superpixels for an image. Recently, an approach called contrastive explanations method (CEM) [6] was proposed which highlights not just correlations or relevances but also features that are minimally sufficient to justify a classification, referred to as pertinent positives (PPs). CEM additionally outputs a minimal set of features, referred to as pertinent negatives (PNs), which when made non-zero or added, alter the classification and thus should remain absent in order for the original classification to prevail. For example, when justifying the classification of a handwritten image of a 3, the method will identify a subset of non-zero or on-pixels within the 3 which by themselves are sufficient for the image to be predicted as a 3 even if all other pixels are turned off (that is, made zero to match background). Moreover, it will identify a minimal set of off-pixels which if turned on (viz. a horizontal line of pixels at the right top making the 3 look like a 5) will alter the classification. Such forms of explanations are not only common in day-to-day social interactions (viz. the twin without the scar) but are also heavily used in fields such as medicine and criminology [6]. [18] notably surveyed 250 papers in social science and philosophy and found contrastive explanations to be among the most important for human explanations.

To identify PNs, addition is easy to define for grayscale images where a pixel with a value of zero indicates no information and so increasing its value towards 1 indicates addition. However, for colored images with rich structure, it is not clear what is a "no information" value for a pixel and consequently what does one mean by addition. Defining addition in a naive way such as simply increasing the pixel or red-green-blue (RGB) channel intensities can lead to uninterpretable images as the relative structure may not be maintained with the added portion being not necessarily interpretable. Moreover, even for grayscale images just increasing values of pixels may not lead to humanly interpretable images nor is there a guarantee that the added portion can be interpreted even if the overall image is realistic and lies on the data manifold.

In this paper, we overcome these limitations by defining "addition" in a novel way which leads to realistic images with the additions also being interpretable. This work is an important contribution toward explaining black-box model predictions because it is applicable to a large class of data sets (whereas [6] was very limited in scope). To showcase the general applicability of our method to various settings, we first experiment with CelebA [17] where we apply our method to a data manifold learned using a generative adversarial network (GAN) [8] trained over the data and by building attribute classifiers for certain high-level concepts (viz. lipstick, hair color) in the dataset. We create realistic images with interpretable additions. Our second experiment is on ISIC Lesions [5, 31] where the data manifold is learned using a variational autoencoder (VAE) [15] and certain (interpretable) latent factors (as no attributes are available) are used to create realistic images with, again, interpretable additions. Latent factors are also learned for a third experiment with Fashion-MNIST [34].

Please note our assumption that high-level interpretable features can be

learned if not given is not the subject of this paper and has been addressed in multiple existing works, e.g., [4, 13]. A key benefit to disentangled representations is interpretability as discussed in [15]. The practicality and interpretability of disentangled features is further validated here by its use in the ISIC Lesions and Fashion-MNIST datasets.

The three usecases show that our method can be applied to colored as well as grayscale images and to datasets that may or may not have high level attributes. It is important to note that our goal is not to generate interpretable models that are understood by humans, but rather to explain why a fixed model outputs a particular prediction. We conducted a human study which concludes that our method offers superior explanations compared to other methods, in particular because our contrastive explanations go beyond visual explanations, which is key to human comprehension.

## 2 Related Work

There have been many methods proposed in literature that aim to explain reasons for their decisions. These methods may be globally interpretable – rule/decision lists [30, 33], or exemplar based – prototype exploration [9, 12], or inspired by psychometrics [10] or interpretable generalizations of linear models [3]. Moreover, there are also works that try to formalize interpretability [7].

A survey by [19] mainly explores two methods for explaining decisions of neural networks: i) Prototype selection methods [21, 22] that produce a prototype for a given class, and ii) Local explanation methods that highlight relevant input features/pixels [1, 14, 25, 28]. Belonging to this second type are multiple local explanation methods that generate explanations for images [23, 24, 29] and some others for NLP applications [16]. There are also works [13] that highlight higher level concepts present in images based on examples of concepts provided by the user. These methods mostly focus on features that are present, although they may highlight negatively contributing features to the final classification. In particular, they do not identify concepts or features that are minimally sufficient to justify the classification or those that should be necessarily absent to maintain the original classification. There are also methods that perturb the input and remove features [27] to verify their importance, but these methods can only evaluate an explanation and do not find one.

Recently, there have been works that look beyond relevance. In [26], the authors try to find features that, with almost certainty, indicate a particular class. These can be seen as global indicators for a particular class. Of course, these may not always exist for a dataset. There are also works [35] that try to find stable insight that can be conveyed to the user in a (asymmetric) binary setting for medium-sized neural networks. The most relevant work to our current endeavour is [6] and, as mentioned before, it cannot be directly applied when it comes to explaining colored images or images with rich structure.

### 3 Methodology

We now describe the methodology for generating contrastive explanations for images. We first describe how to identify PNs, which involves the key contribution of defining "addition" for colored images in a meaningful way. We then describe how to identify PPs, which also utilizes this notion of adding attributes. Finally, we provide algorithmic details for solving the optimization problems in Algorithm 1.

We first introduce some notation. Let  $\mathcal{X}$  denote the feasible input space with  $(\mathbf{x}_0, t_0)$  being an example such that  $\mathbf{x}_0 \in \mathcal{X}$  and  $t_0$  is the predicted label obtained from a neural network classifier. Let  $S$  denote the set of superpixels that partition  $\mathbf{x}_0$  with  $\mathcal{M}$  denoting a set of binary masks which when applied to  $\mathbf{x}_0$  produce images  $\mathcal{M}(x_0)$  by selecting the corresponding superpixels from  $S$ . Let  $M_x$  denote the mask corresponding to image  $\mathbf{x} = M_x(\mathbf{x}_0)$ .

If  $\mathcal{D}(\cdot)$  denotes the data manifold (based on GAN or VAE), then let  $z$  denote the latent representation with  $z_x$  denoting the latent representation corresponding to input  $\mathbf{x}$  such that  $\mathbf{x} = \mathcal{D}(z_x)$ . Let  $k$  denote the number of (available or learned) interpretable features (latent or otherwise) which represent meaningful concepts (viz. moustache, glasses, smile) and let  $g_i(\cdot), \forall i \in \{1, \dots, k\}$ , be corresponding functions acting on these features with higher values indicating presence of a certain visual concept while lower values indicating its absence. For example, CelebA has different high-level (interpretable) features for each image such as whether the person has black hair or high cheekbones. In this case, we could build binary classifiers for each of the features where a 1 would indicate presence of black hair or high cheekbones, while a zero would mean its absence. These classifiers would be the  $g_i(\cdot)$  functions. On the other hand, for datasets with no high-level interpretable features, we could find latents by learning disentangled representations and choose those latents (with ranges) that are interpretable. Here the  $g_i$  functions would be an identity map or negative identity map depending on which direction adds a certain concept (viz. light colored lesion to a dark lesion). We note that these attribute functions could be used as latent features for the generator in a causal graph (e.g., [20]), or given a causal graph for the desired attributes, we could learn these functions from the architecture in [20].

Our procedure for finding PNs and PPs involves solving an optimization problem over the variable  $\delta$  which is the outputted image. We denote the prediction of the model on the example  $\mathbf{x}$  by  $f(\mathbf{x})$ , where  $f(\cdot)$  is any function that outputs a vector of prediction scores for all classes, such as prediction probabilities and logits (unnormalized probabilities) that are widely used in neural networks.

#### 3.1 Pertinent Negatives (PNs)

To find PNs, we want to create a (realistic) image that lies in a different class than the original image but where we can claim that we have (minimally) "added" things to the original image without deleting anything to obtain this new image.

---

**Algorithm 1** Contrastive Explanations Method using Monotonic Attribute Functions (CEM-MAF)

---

**Input:** Example  $(\mathbf{x}_0, t_0)$ , latent representation of  $\mathbf{x}_0$  denoted  $z_{\mathbf{x}_0}$ , neural network classification model  $f(\cdot)$ , set of (binary) masks  $\mathcal{M}$ , and  $k$  monotonic feature functions  $g = \{g_1(\cdot), \dots, g_k(\cdot)\}$ .

1) Solve (1) on example  $(\mathbf{x}_0, t_0)$  and obtain  $\delta^{\text{PN}}$  as the minimizing Pertinent Negative.

2) Solve (2) on example  $(\mathbf{x}_0, t_0)$  and obtain  $\delta^{\text{PP}}$  as the minimizing Pertinent Positive.

return  $\delta^{\text{PN}}$  and  $\delta^{\text{PP}}$ . {Code provided in supplement.}

---

If we are able to do this, we can say that the things that were added, which we call PNs, should be necessarily absent from the original image in order for its classification to remain unchanged.

The question is how to define "addition" for colored or images with rich structure. In [6], the authors tested on grayscale images where intuitively it is easy to define addition as increasing the pixel values towards 1. This, however, does not generalize to images where there are multiple channels (viz. RGB) and inherent structure that leads to realistic images, and where simply moving away from a certain pixel value may lead to unrealistic images. Moreover, addition defined in this manner may be completely uninterpretable. This is true even for grayscale images where, while the final image may be realistic, the addition may not be. The other big issue is that for colored images the background may be any color which indicates no signal and object pixels which are lower in value in the original image if increased towards background will make the object imperceptible in the new image, although the claim would be that we have "added" something. Such counterintuitive cases arise for complex images if we maintain their definition of addition.

Given these issues, we define addition in a novel manner. To define addition we assume that we have high-level interpretable features available for the dataset. Multiple public datasets [17, 36] have high-level interpretable features, while for others such features can be learned using unsupervised methods such as disentangled representations [15] or supervised methods where one learns concepts through labeled examples [13]. Given  $k$  such features, we define functions  $g_i(\cdot), \forall i \in \{1, \dots, k\}$ , as before, where in each of these functions, increasing value indicates addition of a concept. Using these functions, we define addition as introducing more concepts into an image without deleting existing concepts. Formally, this corresponds to never decreasing the  $g_i(\cdot)$  from their original values based on the input image, but rather increasing them. However, we also want a minimal number of additions for our explanation to be crisp and so we encourage as few  $g_i(\cdot)$  as possible to increase in value (within their allowed ranges) that will result in the final image being in a different class. We also want the final image to be realistic and that is why we learn a manifold  $\mathcal{D}$  on which we perturb the image, as we want our final image to also lie on it after the necessary additions.

This gives rise to the following optimization problem:

$$\begin{aligned}
\min_{\boldsymbol{\delta} \in \mathcal{X}} \quad & \gamma \sum_i \max\{g_i(\mathbf{x}_0) - g_i(\mathcal{D}(z_{\boldsymbol{\delta}})), 0\} + \beta \|g(\mathcal{D}(z_{\boldsymbol{\delta}}))\|_1 \\
& - c \cdot \min_{i \neq t_0} \{\max[f(\boldsymbol{\delta})]_i - [f(\boldsymbol{\delta})]_{t_0}, \kappa\} \\
& + \eta \|\mathbf{x}_0 - \mathcal{D}(z_{\boldsymbol{\delta}})\|_2^2 + \nu \|z_{\mathbf{x}_0} - z_{\boldsymbol{\delta}}\|_2^2.
\end{aligned} \tag{1}$$

The first two terms in the objective function here are the novelty for PNs. The first term encourages the addition of attributes where we want the  $g_i(\cdot)$ s for the final image to be no less than their original values. The second term encourages minimal addition of interpretable attributes. The third term is the PN loss from [6] and encourages the modified example  $\boldsymbol{\delta}$  to be predicted as a different class than  $t_0 = \arg \max_i [f(\mathbf{x}_0)]_i$ , where  $[f(\boldsymbol{\delta})]_i$  is the  $i$ -th class prediction score of  $\boldsymbol{\delta}$ . The hinge-like loss function pushes the modified example  $\boldsymbol{\delta}$  to lie in a different class than  $\mathbf{x}_0$ . The parameter  $\kappa \geq 0$  is a confidence parameter that controls the separation between  $[f(\boldsymbol{\delta})]_{t_0}$  and  $\max_{i \neq t_0} [f(\boldsymbol{\delta})]_i$ . The fourth ( $\eta > 0$ ) and fifth terms ( $\nu > 0$ ) encourage the final image to be close to the original image in the input and latent spaces. In practice, one could have a threshold for each of the  $g_i(\cdot)$ , where only an increase in values only beyond that threshold would imply a meaningful addition. The advantage of defining addition in this manner is that not only are the final images interpretable, but so are the additions, and we can clearly elucidate which (concepts) should be necessarily absent to maintain the original classification.

### 3.2 Pertinent Positives (PPs)

To find PPs, we want to highlight a minimal set of important pixels or superpixels which by themselves are sufficient for the classifier to output the same class as the original example. More formally, for an example image  $\mathbf{x}_0$ , our goal is to find an image  $\boldsymbol{\delta} \in \mathcal{M}(x_0)$  such that  $\arg \max_i [\text{Pred}(\mathbf{x}_0)]_i = \arg \max_i [\text{Pred}(\boldsymbol{\delta})]_i$  (i.e. same prediction), with  $\boldsymbol{\delta}$  containing as few superpixels and interpretable concepts from the original image as possible. This leads to the following optimization problem:

$$\begin{aligned}
\min_{\boldsymbol{\delta} \in \mathcal{M}(\mathbf{x}_0)} \quad & \gamma \sum_i \max\{g_i(\boldsymbol{\delta}) - g_i(\mathbf{x}_0), 0\} + \beta \|M_{\boldsymbol{\delta}}\|_1 \\
& - c \cdot \min\{[f(\boldsymbol{\delta})]_{t_0} - \max_{i \neq t_0} [f(\boldsymbol{\delta})]_i, \kappa\}.
\end{aligned} \tag{2}$$

The first term in the objective function here is the novelty for PPs and penalizes the addition of attributes since we seek a sparse explanation. The last term is the PP loss from [6] and is minimized when  $[f(\boldsymbol{\delta})]_{t_0}$  is greater than  $\max_{i \neq t_0} [f(\boldsymbol{\delta})]_i$  by at least  $\kappa \geq 0$ , which is a margin/confidence parameter. Parameters  $\gamma, c, \beta \geq 0$  are the associated regularization coefficients.

In the above formulation, we optimize over superpixels which of course subsumes the case of just using pixels. Superpixels have been used in prior works [25] to provide more interpretable results on image datasets and we allow for this more general option.

<b>Orig. Class</b>	yng, ml, smlg	yng, fml, smlg	yng, fml, not smlg	yng, fml, not smlg	old, ml, not smlg	Mela-noma	Nevus	B. Cell Carc.	B. Kera-tosis	Vasc. Lesion
<b>Orig.</b>										
<b>PN Class</b>	<b>old, fml, smlg</b>	<b>old, fml, smlg</b>	yng, ml, not smlg	yng, fml, <b>smlg</b>	old, ml, <b>smlg</b>	Nevus	Vasc. Lesion	Nevus	Mela-noma	Bas. Cell Carc.
<b>PN</b>										
<b>PN Expl.</b>	+brwn hr, +makeup, +bangs	+oval face	+single hair clr, -bangs	+makeup +oval face	+cheek -bones	rounder	rounder, smaller	rounder, lighter	darker	more oval, smaller
<b>PP</b>										
<b>LIME</b>										
<b>Grad-CAM</b>										

(a) CelebA dataset

(b) ISIC Lesion dataset

Figure 1: CEM-MAF examples on (a) CelebA and (b) ISIC Lesions, both using segmentation with 200 superpixels. Abbreviations are: Orig. for Original, PN for Pertinent Negative, P for Pertinent Positive, and Expl. for Explanation. In (a), change from original class prediction is in bold in PN class prediction. Abbreviations in class predictions are as follows: yng for young, ml for male, fml for female, smlg for smiling. In (b), change from original prediction is based on change in disentangled features.

### 3.3 Optimization Details

To solve for PNs as formulated in (1), we note that the  $L_1$  regularization term is penalizing a non-identity and complicated function  $\|g(\mathcal{D}(z_\delta))\|_1$  of the optimization variable  $\delta$  involving the data manifold  $\mathcal{D}$ , so proximal methods are not applicable. Instead, we use 1000 iterations of standard subgradient descent to solve (1). We find a PN by setting it to be the iterate having the smallest  $L_2$  distance  $\|z_{\mathbf{x}_0} - z_\delta\|_2$  to the latent code  $z_{\mathbf{x}_0}$  of  $\mathbf{x}_0$ , among all iterates where the prediction score of solution  $\delta^*$  is at least  $[f(\mathbf{x}_o)]_{t_0}$ .

To solve for PPs as formulated in (2), we first relax the binary mask  $M_\delta$  on superpixels to be real-valued (each entry is between  $[0, 1]$ ) and then apply the standard iterative soft thresholding algorithm (ISTA) (see [2] for various references) that efficiently solves optimization problems with  $L_1$  regularization. We run 100 iterations of ISTA in our experiments and obtain a solution  $M_{\delta^*}$  that has the smallest  $L_1$  norm and satisfies the prediction of  $\delta^*$  being within margin  $\kappa$  of  $[f(\mathbf{x}_o)]_{t_0}$ . We then rank the entries in  $M_{\delta^*}$  according to their values in descending order and subsequently add ranked superpixels until the masked image predicts  $[f(\mathbf{x}_o)]_{t_0}$ .

A discussion of hyperparameter selection is held to the Supplement.

## 4 Experiments

We next illustrate the usefulness of CEM-MAF on two image data sets - CelebA [17] and ISIC Lesions [5, 31] (results on Fashion-MNIST [34] are in the Supplement). These datasets cover the gamut of images having known versus derived features. CEM-MAF handles each scenario and offers explanations that are understandable by humans. These experiments exemplify the following observations:

- PNs offer intuitive explanations given a set of interpretable monotonic attribute functions. In fact, our user study finds them to be the preferred form of explanation since describing a decision in isolation (viz. why is a smile a smile) using PPs, relevance, or heatmaps is not always informative.
- PPs offer better direction as to what is important for the classification versus too much direction by LIME (shows too many features) or too little direction by Grad-CAM (only focuses on smiles).
- PPs and PNs offer the guarantee of being 100% accurate in maintaining or changing the class respectively as seen in Table 1 versus LIME or Grad-CAM.
- Both proximity in the input and latent space along with sparsity in the additions play an important role in generating good quality human-understandable contrastive explanations.

### 4.1 CelebA with Available High-Level Features

CelebA is a large-scale dataset of celebrity faces annotated with 40 attributes [17].

#### 4.1.1 Setup

The CelebA experiments explain an 8-class classifier learned from the following binary attributes: Young/Old, Male/Female, Smiling/Not Smiling. We train a Resnet50 [11] architecture to classify the original CelebA images. We selected the following 11 attributes as our  $\{g_i\}$  based on previous studies [15] as well as based on what might be relevant for our class labels: High Cheekbones, Narrow Eyes, Oval Face, Bags Under Eyes, Heavy Makeup, Wearing Lipstick, Bangs, Gray Hair, Brown Hair, Black Hair and Blonde Hair. Note that this list does not include the attributes that define the classes because an explanation for someone that is smiling which simply says they are smiling would not be useful. See Supplement for details on training these attribute functions and the GAN used for generation.



Table 1: Quantitative comparison of CEM-MAF, LIME, and Grad-CAM on the CelebA and ISIC Lesions datasets. Results for Fashion-MNIST with similar patterns can be found in the Supplement.

Dataset	Method	# PP Feat	PP Acc	PP Corr
CelebA	CEM-MAF	16.0	100	-.742
	LIME	75.1	30	.035
	Grad-CAM	17.6	30	.266
ISIC Lesions	CEM-MAF	66.7	100	-.976
	LIME	108.3	100	-.986
	Grad-CAM	95.6	50	-.772

#### 4.1.2 Observations

Results on five images are exhibited in Figure 1 (a) using a segmentation into 200 superpixels (more examples in Supplement). The first two rows show the original class prediction followed by the original image. The next two rows show the pertinent negative’s class prediction and the pertinent negative image. The fourth row lists the attributes that were modified in the original, i.e., the reasons why the original image is not classified as being in the class of the pertinent negative. The next row shows the pertinent positive image, which combined with the PN, gives the complete explanation. The final two rows illustrate different explanations that can be compared with the PP: one derived from locally interpretable model-agnostic explanations (LIME) [25] followed by a gradient-based localized explanation designed for CNN models (Grad-CAM) [24].

First consider class explanations given by the PPs. Age seems to be captured by patches of skin, sex by patches of hair, and smiling by the presence or absence of the mouth. One might consider the patches of skin to be used to explain young versus old. PPs capture a part of the smile for those smiling, while leave out the mouth for those not smiling. Visually, these explanations are simple (very few selected features) and useful although they require human analysis. In comparison, LIME selects many more features that are relevant to the prediction, and while also useful, requires even more human intervention to explain the classifier. Grad-CAM, which is more useful for discriminative tasks, seems to focus on the mouth and does not always find a part of the image that is positively relevant to the prediction.

A performance comparison of PPs between CEM-MAF, LIME, and Grad-CAM is given in Table 1. Across colored images, CEM-MAF finds a much sparser subset of superpixels than LIME and is guaranteed to have the same prediction as the original image. Both LIME and Grad-CAM select features for visual explanations that often have the wrong prediction (low PP accuracy). A third measure, PP Correlation, measures the benefit of each additional feature by ranking the prediction scores after each feature is added (confidence in the

prediction should increase) and correlating with the expected ranks (perfect correlation here would give -1). Order for LIME was determined by classifier weights while order for Grad-CAM was determined by colors in the corresponding heatmaps. CEM-MAF is best or on par at selecting features that increase confidence.

More intuitive explanations are offered by the pertinent negatives in Figure 1. The first PN changes a young, smiling, male into an old, smiling, female by adding a second hair color, makeup, and bangs. Younger age more likely corresponds to a single hair, and being male is explained by a lack of makeup or bangs, more associated with females. Another way to explain young age is the absence of an oval face in the second column. The third PN changes a female into a male, and the female is explained by the absence of a single hair color (in fact, she has black hair with brown highlights) and the presence of bangs. While the presence of bangs is intuitive, it is selected because our constraints of adding features to form PNs can be violated due to enforcing the constraints with regularization. The last two columns explain a face not smiling by the absence of high cheekbones or the absence of an oval face (since your face can become more oval when you raise your cheekbones).

Note that the first example where the male was changed to a female in the PN was obtained by regularizing only the latent representation proximity. Our framework allows for different regularizations, and in fact, regularizing sparsity in the number of attributes for this example results in a PN with only a single, rather than three, added attributes classified as a young male that is not smiling (image in Supplement).

## 4.2 Skin Lesions with Learned Disentangled Features

The International Skin Imaging Collaboration (ISIC) Archive (<https://challenge2018.isic-archive.com/>) is a large-scale image dataset consisting of dermoscopic (special photographic technique for removing surface reflections) images of skin lesions [5, 31]. Descriptions of the seven different types of lesions can be found in the Supplement.

### 4.2.1 Setup

For ISIC Lesions, we explain a 7-class classifier trained on a Resnet9 architecture (classes such as melanoma, nevus, etc.). As with CelebA, we train a VAE to generate realistic images for PNs. However, this data does not have annotated features as in CelebA, so we learn the features using disentanglement following a recent variant of VAE called DIP-VAE [15] (see Supplement for more details).

We can then use these disentangled latent features in lieu of the ground truth attributes. Based on what might be relevant to the categories of skin lesions, we use ten dimensions from the latent code as attributes, corresponding to size, roundness, darkness, and border definition. Figure 2 visualizes features corresponding to increasing size and shape change from circular to oval as the

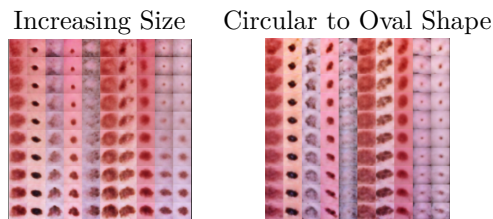


Figure 2: Qualitative results for disentanglement of ISIC Lesions images. Full visualization is in the Supplement.

features increase. A visualization of all disentangled features, ISIC Lesions and Fashion-MNIST, can be found in the Supplement.

#### 4.2.2 Observations

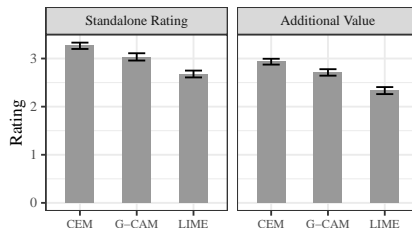
Results on five images are exhibited in Figure 1 (b), also using a segmentation into 200 superpixels (more examples in the Supplement). Rows here are the same as described above for CelebA. Explanations for the PPs can be determined using descriptions of the lesions. The first PP for an image of Melanoma leaves parts of the lesion displaying two different colors, black and brown (these lesions usually do not have a single solid color). The third PP of Basal Cell Carcinoma highlights the pink and skin color associated with the most common type of such lesions (and removes the border meaning the prediction does not focus on the border). LIME highlights similar areas, while using more superpixels. Grad-CAM mostly does not highlight specific areas of the lesions, but rather the entire lesion. Grad-CAM removes the brown part of the first Melanoma and the resulting prediction is incorrect (Melanoma usually does not have a single solid color). Note that Nevus lesion PPs contain a single superpixel due to heavy dataset bias for this class.

The contrastive explanations offered by the PNs offer much more intuition. For example, the first lesion is classified as a Melanoma because it is not rounder, in which case it would be classified as a Nevus (the PN). In fact, Melanomas are known to be asymmetrical due to the quick and irregular growth of cancer cells in comparison to normal cells. In the fourth column, the Benign Keratosis lesion is classified as such because it is not darker, in which case it would be classified as a Melanoma (the darker center creates the multi-colored lesion associated with Melanoma)

## 5 User Study

In order to further illustrate the usefulness of, and preference for, contrastive explanations, we conducted a thorough user study comparing CEM-MAF, LIME, and Grad-CAM. Our study assesses two questions: are the explanations useful by themselves and whether or not an additional explanation would add to

CEM-MAF vs Grad-CAM vs LIME



PN vs PP vs Grad-CAM vs LIME

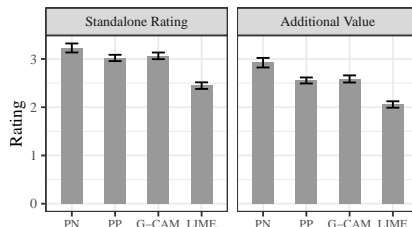


Figure 3: User study results. Top figures compare CEM-MAF with Grad-CAM (G-CAM) and LIME, where figure (left) rates the usefulness of explanations while figure (right) rates additional value given one of the other explanations. Bottom figures show similar ratings but separates CEM-MAF into PN and PP. Error bars show standard error.

the usefulness of an initial explanation. LIME and Grad-CAM clearly have usefulness as explanation methods, evidenced by previous literature. Contrastive explanations offer different information that could be viewed as complimentary to the visual explanations given by the other methods. Pertinent positives, while also visual, have a specific meaning in highlighting a minimally sufficient part of the image to obtain a classifier’s prediction, while LIME highlights significant features using local linear classifiers and Grad-CAM highlights features that attribute maximum change to the prediction. Each method provides different information. Pertinent negatives illuminate a completely different aspect that is known to be intuitive to humans [18], and importantly does not require humans to interpret what is learned since the method outputs exactly what modifications are necessary to change the prediction.

The study was conducted on Amazon Mechanical Turk using CelebA images. A single trial of the study proceeds as follows. An original image is displayed along with the model’s prediction in a sentence, e.g., “The system thinks the image shows a young male who is smiling.” Under the image, one of the three explanation methods, titled “Explanation 1” for anonymity, is displayed with a brief description of the explanation, e.g. “The colored pixels highlight the parts of the original image that may have contributed significantly to the system’s recognition result.” The question, “Is the explanation useful?”, is posed next to Explanation 1 along with five choices ranging from “I don’t understand

the explanation" to "I understand the explanation and it helps me completely understand what features the system used to recognize a young, male, who is smiling" (the words for the prediction change per image).

After answering the first question, another image, titled "Explanation 2", is displayed under the first explanation, again with a short blurb about what the explanation exhibits. If the first explanation was LIME, the second explanation would be CEM-MAF or Grad-CAM. The question posed next to this explanation is "How much does adding the second explanation to the first improve your understanding of what features the system used to recognize a young male who is smiling?" There are five possible responses ranging from "None" to "Completes my understanding." In a second survey, we ask the same questions for four methods, where we separate CEM-MAF and pose the pertinent positive and pertinent negative as two different explanations. A screenshot of a single trial can be found at the end of the Supplement.

Each user in the study is required to spend at least 30 seconds reading a page of instructions that gives examples of the three (or four) possible explanations and explains what will be asked during the survey. Then each user proceeds through 24 trials as described above. Each of the three methods is assigned to both explanations 1 and 2 such that a user sees each of the six permutations four times (the second survey with four explanations has twelve permutations that are each seen twice). Each trial draws a random image from a batch of 76 images for which we have ran all methods. As LIME requires tuning, we restrict LIME to use the same number of superpixels as used in the pertinent positives for an apples-to-apples comparison. Regarding demographics, we attempt to run the survey over a population that is more likely to use the methods of this paper by restricting job function of participants to Information Technology. Each survey was taken by 100 different participants (200 total), 157 males vs 40 females (remaining declined), with 81 people aged 30-39 (full age table in Supplement).

Results are displayed in Figure 3. The standalone ratings judge individual usefulness of all explanation methods. CEM-MAF has a clear, albeit, slight advantage in terms of usefulness over other methods, and when broken down, it is apparent that the usefulness is driven more by the PN than the PP, which is on par with Grad-CAM. The direct explanation that requires no human intervention to interpret the explanation seems to be most useful (i.e., PNs directly output via text what the explanation is whereas other methods require a human to interpret what is understood visually). Given one explanation, the additional value of offering a second explanation follows a similar pattern to the standalone ratings. This means that users given a Grad-CAM or LIME explanation found the contrastive explanation to offer more additional understanding than if they were first given CEM-MAF followed by Grad-CAM or LIME. Note these results are averaged, for example, with CEM-MAF as the second explanation, over all trials with either Grad-CAM or LIME as the first explanation.

While CEM-MAF was observed as the most useful explanation, comments made at the end of the survey suggest what has been mentioned earlier: each of the different explanation methods have value. Such comments included "The explanations were straightforward" and "I thought they were pretty accurate

overall and helped in the decision making process". Other comments suggested that there is still much variability in the success of explanation methods, e.g., "I thought they were very unique and amazing to see. I thought the explanations were usually a bit confused, but some were very advanced" and "The explanation made sense to me, though I think some of them were lacking in complexity and detail." Such comments also point out where contrastive explanations can have major impact. For example, since PP's dictate, by definition, when a classifier requires very little information to make its prediction (i.e., require "little complexity and detail"), they can be used to locate classifiers that should be reassessed prior to deployment.

## 6 Discussion

In this paper, we leveraged high-level features that were readily available (viz. CelebA) as well as used generated ones (viz. ISIC Lesions and Fashion-MNIST) based on unsupervised methods to produce contrastive explanations. As mentioned before, one could also learn interpretable features in a supervised manner as done in [13] which we could also use to generate such explanations. Regarding learning the data manifold, it is important to note that we do not need a global data manifold to create explanations; a good *local* data representation around the image should be sufficient. Thus, for datasets where building an accurate global representation may be hard, a good local representation (viz. using conditional GANs) should make it possible to generate high quality contrastive explanations.

Several future directions are motivated by the user study. Extracting text to describe highlighted aspects of visual explanations (PP, LIME, and Grad-CAM) could better help their understanding by humans. As previously mentioned, an important feature of contrastive explanations is that they can be used to identify classifiers that should not be trusted. PP's composed of two superpixels in our CelebA experiments could identify examples where the classifier requires little relevant information, and hence might not be operating in a meaningful way. The study reinforced this concept because users found visual explanations with few superpixels to be less useful. Studying this relationship between human trust and contrastive explanations is an interesting direction.

In summary, we have proposed a method to create contrastive explanations for image data with rich structure. The key novelty over previous work is how we define addition, which leads to realistic images where added information is easy to interpret (e.g., added makeup). Our results showcase that using pertinent negatives might be the preferred form of explanation where it is not clear why a certain entity is what it is in isolation (e.g. based on relevance or pertinent positives), but could be explained more crisply by contrasting it to another entity that closely resembles it (viz. adding high cheekbones to a face makes it look smiling).

## References

- [1] Sebastian Bach, Alexander Binder, Grégoire Montavon, Frederick Klauschen, Klaus-Robert Müller, and Wojciech Samek. On pixel-wise explanations for non-linear classifier decisions by layer-wise relevance propagation. *PloS one*, 10(7):e0130140, 2015.
- [2] Amir Beck and Marc Teboulle. A fast iterative shrinkage-thresholding algorithm for linear inverse problems. *SIAM journal on imaging sciences*, 2(1):183–202, 2009.
- [3] Rich Caruana, Yin Lou, Johannes Gehrke, Paul Koch, Marc Sturm, and Noemie Elhadad. Intelligible models for healthcare: Predicting pneumonia risk and hospital 30-day readmission. In *KDD 2015*, pages 1721–1730, New York, NY, USA, 2015. ACM.
- [4] Xi Chen, Yan Duan, Rein Houthoofd, John Schulman, Ilya Sutskever, and Pieter Abbeel. Infogan: Interpretable representation learning by information maximizing generative adversarial nets. In *Advances in Neural Information Processing Systems*, 2016.
- [5] N. Codella, V. Rotemberg, P. Tschandl, M. E. Celebi, S. Dusza, D. Gutmanand B. Helba, A. Kalloo, K. Liopyris, M. Marchetti, H. Kittler, and A. Halpern. Skin lesion analysis toward melanoma detection 2018: A challenge hosted by the international skin imaging collaboration (isic). In <https://arxiv.org/abs/1902.03368>, 2018.
- [6] Amit Dhurandhar, Pin-Yu Chen, Ronny Luss, Chun-Chen Tu, Paishun Ting, Karthikeyan Shanmugam, and Payel Das. Explanations based on the missing: Towards contrastive explanations with pertinent negatives. In *NeurIPS 2018*, 2018.
- [7] Amit Dhurandhar, Vijay Iyengar, Ronny Luss, and Karthikeyan Shanmugam. Tip: Typifying the interpretability of procedures. *arXiv preprint arXiv:1706.02952*, 2017.
- [8] I. Goodfellow, Y. Bengio, and A. Courville. *Deep Learning*. MIT Press, 2016.
- [9] Karthik Gurumoorthy, Amit Dhurandhar, and Guillermo Cecchi. Protodash: Fast interpretable prototype selection. *arXiv preprint arXiv:1707.01212*, 2017.
- [10] Tsuyoshi Idé and Amit Dhurandhar. Supervised item response models for informative prediction. *Knowl. Inf. Syst.*, 51(1):235–257, April 2017.
- [11] Shaoqing Ren Kaiming He, Xiangyu Zhang and Jian Sun. Deep residual learning for image recognition. In *CVPR 2016*, June 2016.

- [12] Been Kim, Rajiv Khanna, and Oluwasanmi Koyejo. Examples are not enough, learn to criticize! criticism for interpretability. In *In Advances of Neural Inf. Proc. Systems*, 2016.
- [13] Been Kim, Martin Wattenberg, Justin Gilmer, Carrie Cai, James Wexler, Fernanda Viegas, and Rory Sayres. Interpretability beyond feature attribution: Quantitative testing with concept activation vectors. *Intl. Conf. on Machine Learning*, 2018.
- [14] Pieter-Jan Kindermans, Kristof T. Schütt, Maximilian Alber, Klaus-Robert Müller, Dumitru Erhan, Been Kim, and Sven Dähne. Learning how to explain neural networks: Patternnet and patternattribution. In *Intl. Conference on Learning Representations (ICLR)*, 2018.
- [15] Abhishek Kumar, Prasanna Sattigeri, and Avinash Balakrishnan. Variational inference of disentangled latent concepts from unlabeled observations. *Intl. Conf. on Learning Representations*, 2017.
- [16] Tao Lei, Regina Barzilay, and Tommi Jaakkola. Rationalizing neural predictions. *arXiv preprint arXiv:1606.04155*, 2016.
- [17] Ziwei Liu, Ping Luo, Xiaogang Wang, and Xiaoou Tang. Deep learning face attributes in the wild. In *ICCV 2015*, December 2015.
- [18] Tim Miller. Contrastive explanation: A structural-model approach. *CoRR*, abs/1811.03163, 2018.
- [19] Grégoire Montavon, Wojciech Samek, and Klaus-Robert Müller. Methods for interpreting and understanding deep neural networks. *Digital Signal Processing*, 2017.
- [20] Alexandros G. Dimakis Murat Kocaoglu Christopher Snyder and Sriram Vishwanath. Causalgan: Learning causal implicit generative models with adversarial training. In *ICLR 2018*, 2018.
- [21] Anh Nguyen, Alexey Dosovitskiy, Jason Yosinski, Thomas Brox, and Jeff Clune. Synthesizing the preferred inputs for neurons in neural networks via deep generator networks. In *NIPS*, 2016.
- [22] Anh Nguyen, Jason Yosinski, and Jeff Clune. Multifaceted feature visualization: Uncovering the different types of features learned by each neuron in deep neural networks. *arXiv preprint arXiv:1602.03616*, 2016.
- [23] Jose Oramas, Kaili Wang, and Tinne Tuytelaars. Visual explanation by interpretation: Improving visual feedback capabilities of deep neural networks. In *arXiv:1712.06302*, 2017.
- [24] Abhishek Das Ramakrishna Vedantam Devi Parikh Ramprasaath R. Selvaraju, Michael Cogswell and Dhruv Batra. Grad-cam: Visual explanations from deep networks via gradient-based localization. In *ICCV*, October 2017.



- [25] Marco Ribeiro, Sameer Singh, and Carlos Guestrin. "why should i trust you?" explaining the predictions of any classifier. In *KDD 2016*, 2016.
- [26] Marco Tulio Ribeiro, Sameer Singh, and Carlos Guestrin. Anchors: High-precision model-agnostic explanations. In *AAAI 2018*, 2018.
- [27] Wojciech Samek, Alexander Binder, Grégoire Montavon, Sebastian Lapuschkin, and Klaus-Robert Müller. Evaluating the visualization of what a deep neural network has learned. In *IEEE TNNLS*, 2017.
- [28] Su-In Lee Scott Lundberg. Unified framework for interpretable methods. In *NIPS 2017*, 2017.
- [29] Karen Simonyan, Andrea Vedaldi, and Andrew Zisserman. Deep inside convolutional networks: Visualising image classification models and saliency maps. *CoRR*, abs/1312.6034, 2013.
- [30] Guolong Su, Dennis Wei, Kush Varshney, and Dmitry Malioutov. Interpretable two-level boolean rule learning for classification. In <https://arxiv.org/abs/1606.05798>, 2016.
- [31] P. Tschandl, C. Rosendahl, and H. Kittler. The ham10000 dataset, a large collection of multi-source dermatoscopic images of common pigmented skin lesions. *Sci. Data*, 5, 2018.
- [32] Kush Varshney. Engineering safety in machine learning. In <https://arxiv.org/abs/1601.04126>, 2016.
- [33] Fulton Wang and Cynthia Rudin. Falling rule lists. In *In AISTATS*, 2015.
- [34] Han Xiao, Kashif Rasul, and Roland Vollgraf. Fashion-mnist: a novel image dataset for benchmarking machine learning algorithms. *CoRR*, abs/1708.07747, 2017.
- [35] Xin Zhang, Armando Solar-Lezama, and Rishabh Singh. Interpreting neural network judgments via minimal, stable, and symbolic corrections. 2018. <https://arxiv.org/abs/1802.07384>.
- [36] Shi Qiu Xiaogang Wang Ziwei Liu, Ping Luo and Xiaoou Tang. Deepfashion: Powering robust clothes recognition and retrieval with rich annotations. In *CVPR 2016*, June 2016.

## Supplement

Note all model training for experiments is done using Tensorflow and Keras.

### 1 Hyperparameter selection for PN and PP

Finding PNs is done by solving (1) which has hyperparameters  $\kappa, \gamma, \beta, \eta, \mu, c$ . The confidence parameter  $\kappa$  is the user’s choice. We experimented with  $\kappa \in \{0.5, 5.0\}$  and report results with  $\kappa = 5.0$ . We experimented with  $\gamma \in \{1, 100\}$  and report results with  $\gamma = 100$  which better enforces the constraint of only adding attributes to a PN. The three hyperparameters  $\beta = 100, \eta = 1.0, \nu = 1.0$  were fixed. Sufficient sparsity in attributes was obtained with this value of  $\beta$  but further experiments increasing  $\beta$  could be done to allow for more attributes if desired. The results with selected  $\eta$  and  $\nu$  were deemed realistic there so there was no need to further tune them. Note that CelebA PN experiments required experimenting with  $\beta = 0$  to remove the attribute sparsity regularization. The last hyperparameter  $c$  was selected via the following search: Start with  $c = 1.0$  and multiply  $c$  by 10 if no PN found after 1000 iterations of subgradient descent, and divided by 2 if PN found. Then run the next 1000 iterations and update  $c$  again. This search on  $c$  was repeated 9 times, meaning a total of  $1000 \times 9 = 9000$  iterations of subgradient descent were run with all other hyperparameters fixed.

Finding PPs is done by solving (2) which has hyperparameters  $\kappa, \gamma, \beta, c$ . Again, we experimented with  $\kappa \in \{0.5, 5.0\}$  and report results with  $\kappa = 5.0$ . We experimented with  $\gamma \in \{1, 100\}$  and report results with  $\gamma = 100$  for the same reason as for PNs. The hyperparameter  $\beta = 0.1$  because  $\beta = 100$  as above was too strong and did not find PPs with such high sparsity (usually allowing no selection). The same search on  $c$  as described for PNs above was done for PPs, except this means a total of  $9 \times 100$  iterations of ISTA were run with all other hyperparameters fixed to learn a single PP.

### 2 Additional CelebA Information

We here discuss how attribute classifiers were trained for CelebA, describe the GAN used for generation, and provide additional examples of CEM-MAF. CelebA datasets are available at <http://mmlab.ie.cuhk.edu.hk/projects/CelebA.html>.

#### 2.1 Training attribute classifiers for CelebA

For each of the 11 selected binary attributes, a CNN with four convolutional layers followed by a single dense layer was trained on 10000 CelebA images with Tensorflow’s SGD optimizer with Nesterov using learning rate=0.001, decay=1e-6, and momentum=0.9. for 250 epochs. Accuracies of each classifiers are given in Table 2.

Table 2: CelebA binary attribute classifier accuracies on 1000 test images

<b>Attribute</b>	<b>Accuracy</b>
High Cheekbones	84.5%
Narrow Eyes	78.8%
Oval Face	63.7%
Bags Under Eyes	79.3%
Heavy Makeup	87.9%
Wearing Lipstick	90.6%
Bangs	93.0%
Gray Hair	93.5%
Brown Hair	76.3%
Black Hair	86.5%
Blonde Hair	93.1%

## 2.2 GAN Information

Our setup processes each face as a  $224 \times 224$  pixel colored image. A GAN was trained over the CelebA dataset in order to generate new images that lie in the same distribution of images as CelebA. Specifically, we use the pretrained progressive GAN<sup>1</sup> to approximate the data manifold of the CelebA dataset. The progressive training technique is able to grow both the generator and discriminator from low to high resolution, generating realistic human face images at different resolutions.

## 2.3 Additional CelebA Examples

Figure 4 (a) gives additional examples of applying CEM-MAF to CelebA. Similar patterns can be seen with the PPs. CEM-MAF provides sparse explanations highlighting a few features, LIME provides explanations (positively relevant superpixels) that cover most of the image, and Grad-CAM focuses on the mouth area.

## 3 Additional ISIC Lesions Information

We here discuss what the different types of lesions in the ISIC dataset are, how disentangled features were learned for ISIC lesions, and provide additional examples of CEM-MAF. The ISIC Lesions dataset is available at <https://challenge2018.isic-archive.com/>.

<sup>1</sup>[https://github.com/tkarras/progressive\\_growing\\_of\\_gans](https://github.com/tkarras/progressive_growing_of_gans)

Original Class Pred	old, fml, not smlg	yng, fml, smlg	yng, fml, smlg	yng, ml, smlg	yng, fml, not smlg	Nevus	Nevus	A. Kera, -tosis	B. Kera, -tosis	Vasc., Lesion
Original										
Pert. Neg. Class Pred	<b>yng, fml, smlg</b>	<b>yng, fml, not smlg</b>	<b>yng, ml, smlg</b>	<b>yng, ml, not smlg</b>	<b>old, fml, smlg</b>	Mela-noma	B. Kera, -tosis	Nevis	B. Cell, Carc.	Nevis
Pertinent Negative										
Pertinent Positive										
LIME										
Grad-CAM										

(a) CelebA dataset

(b) ISIC Lesion dataset

Figure 4: Additional CEM-MAF examples on CelebA (a) and ISIC Lesions (b) using segmentation with 200 superpixels. Change from original class prediction is in bold in PN class prediction for CelebA. Abbreviations in class predictions are as follows: yng for young, ml for male, fml for female, smlg for smiling. For ISIS Lesions, change from original prediction is based on change in disentangled features.

### 3.1 Lesion Descriptions

The ISIC dataset is composed of dermoscopic images of lesions classified into the following seven categories: Melanoma, Melanocytic Nevus, Basal Cell Carcinoma, Actinic Keratosis, Benign Keratosis, Dermatofibroma, and Vascular Lesions. Information about these categories is available at <https://challenge2018.isic-archive.com/> but we give some key information about these lesions below. All description were obtained from [www.healthline.com/health](http://www.healthline.com/health).

**Melanoma:** Cancerous mole, asymmetrical due to cancer cells growing more quickly and irregularly than normal cells, fuzzy border, different shades of same color or splotches of different color (but not one solid color). Many different tests to diagnose the stage of cancer.

**Melanocytic Nevus:** Smooth, round or oval-shaped mole. Usually raised, single or multi-colored, might have hairs growing out. Pink, tan, or brown. Might need biopsy to rule out skin cancer.

**Basal Cell Carcinoma:** At least 5 types, pigmented (brown, blue, or black lesion with translucent and raised border), superficial (reddish patch on the skin, often flat and scaly, continues to grow and often has a raised edge), nonulcerative (bump on the skin that is white, skin-colored, or pink, often translucent, with blood vessels underneath that are visible, most common type of BCC), morpheaform (least common type of BCC, typically resembles a scarlike

lesion with a white and waxy appearance and no defined border), basosquamous (extremely rare).

**Actinic Keratosis:** Typically flat, reddish, scale-like patch often larger than one inch. Can start as firm, elevated bump, or lump. Skin patch can be brown, tan, gray, or pink. Visual diagnosis, but skin biopsy necessary to rule out change to cancer.

**Benign Keratosis:** Starts as small, rough, area, usually round or oval-shaped. Usually brown, but can be yellow, white, or black. Usually diagnosed by eye.

**Dermatofibroma:** Small, round noncancerous growth, different layers. Usually firm to the touch. Usually a visual diagnosis.

**Vascular Lesions:** \*Too many types to list.

### 3.2 Learning Disentangled Features for ISIC Lesions

Our setup processes each item as a  $128 \times 128$  pixel color image. As with many real-world scenarios, ISIC Lesion samples come without any supervision about the generative factors or attributes. For such data, we can rely on latent generative models such as VAE that aim to maximize the likelihood of generating new examples that match the observed data. VAE models have a natural inference mechanism baked in and thus allow principled enhancement in the learning objective to encourage disentanglement in the latent space. For inferring disentangled factors, inferred prior or expected variational posterior should be factorizable along its dimensions. We use a recent variant of VAE called DIP-VAE [15] that encourages disentanglement by explicitly matching the inferred aggregated posterior to the prior distribution. This is done by matching the covariance of the two distributions which amounts to decorrelating the dimensions of the inferred prior. Table 3 details the architecture for training DIP-VAE on ISIC Lesions.

Figure 5 shows the disentanglement in these latent features by visualizing the VAE decoder’s output for single latent traversals (varying a single latent between  $[-3, 3]$  while keeping others fixed). For example, we can see that increasing the value of the third dimension (top row) of the latent code corresponds to changing from circular to oval while increasing the value of the fourth dimension (top row) corresponds to decreasing size.

Table 3: Details of the model architecture used for training DIP-VAE [15] on ISIC Lesions.

Architecture	
Input	16384 (flattened 128x128x1)
Encoder	Conv 32x4x4 (stride 2), 32x4x4 (stride 2), 64x4x4 (stride 2), 64x4x4 (stride 2), FC 256. ReLU activation
Latents	32
Decoder	Deconv reverse of encoder. ReLU activation. Gaussian

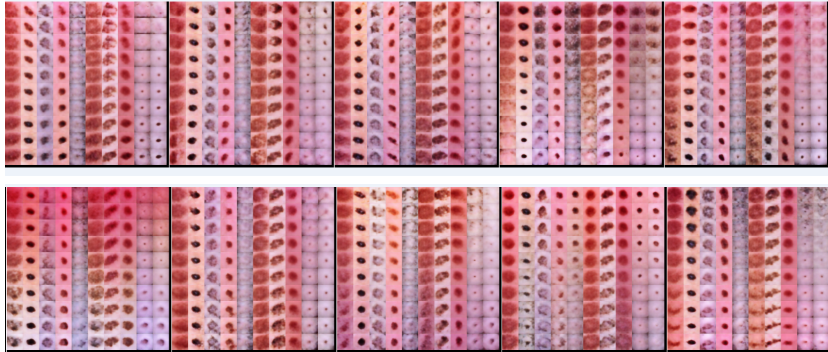


Figure 5: Qualitative results for disentanglement in the ISIC Lesions dataset. The figure shows the DIP-VAE decoder’s output for single latent traversals (varying a single latent between  $[-3, 3]$  while keeping others fixed). Each row show 5 unique features separated by bold black lines.

## 4 Fashion-MNIST with Disentangled Features

Fashion-MNIST is a large-scale image dataset of various fashion items (e.g., coats, trousers, sandals). We here discuss how disentangled features were learned for Fashion-MNIST, how classifiers were trained, and provide additional examples of CEM-MAF. Fashion-MNIST datasets are available at <https://github.com/zalando-research/fashion-mnist>.

### 4.0.1 Learning Disentangled Features for Fashion-MNIST

Two datasets are created as subsets of Fashion-MNIST, one for clothes (tee-shirts, trousers, pullovers, dresses, coats, and shirts) and one for shoes (sandals, sneakers, and ankleboots). Our setup processes each item as a  $28 \times 28$  pixel grayscale image. Again, a VAE was trained to learn the Fashion-MNIST manifold, and we again learn the features using DIP-VAE due to a lack of annotated features. Table 4 details the architecture for training DIP-VAE on Fashion-MNIST.

Based on what might be relevant to the clothes and shoes classes, we use four dimensions from the latent codes corresponding to sleeve length, shoe mass, heel length and waist size. Given these attributes, we learn two classifiers, one with six classes (clothes) and one with three classes (shoes).

Figure 6 shows the disentanglement in these latent features by visualizing the VAE decoder’s output for single latent traversals (varying a single latent between  $[-3, 3]$  while keeping others fixed). For example, we can see that increasing the value of the second dimension  $z_2$  of the latent code corresponds to increasing sleeve length while increasing the value of the third dimension  $z_3$  corresponds to adding more material on the shoe.

Table 4: Details of the model architecture used for training DIP-VAE [15] on Fashion-MNIST.

	<b>Architecture</b>
Input	784 (flattened 28x28x1)
Encoder	FC 1200, 1200. ReLU activation.
Latents	16
Decoder	FC 1200, 1200, 1200, 784. ReLU activation.
Optimizer	Adam (lr = 1e-4) with mse loss

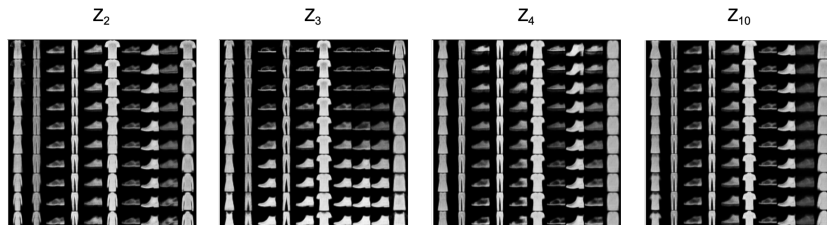


Figure 6: Qualitative results for disentanglement in Fashion MNIST dataset. The figure shows the DIP-VAE decoder’s output for single latent traversals (varying a single latent between  $[-3, 3]$  while keeping others fixed). The title of each image grid denotes the dimension of the latent code that was varied.

## 4.1 Training Fashion-MNIST classifiers

Two datasets are created as subsets of Fashion-MNIST, one for clothes (tee-shirts, trousers, pullovers, dresses, coats, and shirts) and one for shoes (sandals, sneakers, and ankleboots). We train CNN models for each of these subsets with two convolutional layers followed by two dense layer to classify corresponding images from original Fashion-MNIST dataset. See Table 5 for training details.

### 4.1.1 Observations

Results on ten clothes images and ten shoe images are shown in Figure 7 (a) and (b), respectively. In order to make a fair comparison with CEM, we do not segment the images but rather do feature selection pixel-wise. Note that CEM does not do pixel selection for PPs but rather modifies pixel values.

Let us first look at the PPs. They are mostly sparse explanations and do not give any visually intuitive explanations. Both LIME and Grad-CAM, by selecting many more relevant pixels, offers a much more visually appealing explanation. However, these explanations simply imply, for example, that the shirt in the first row of Figure 7 (a) is a shirt because it looks like a shirt. These two datasets (clothes and shoes) are examples where the present features do not offer an intuitive explanation. Table 1 again shows that CEM-MAF selects much fewer

Table 5: Details of the model architecture used for training classifiers on Fashion-MNIST.

	<b>Architecture</b>
Input	28x28x1
Shoes Classifier	Conv (5,5,32), MaxPool(2,2), Conv(5,5,64), MaxPool(2,2), Flatten, FC 1024, Dropout (rate=0.4), FC 3, Relu activation.
Clothes Classifier	Conv (5,5,32), MaxPool(2,2), Conv(5,5,64), MaxPool(2,2), Flatten, FC 1024, Dropout (rate=0.4), FC 6, Relu activation.
Optimizer	SGD (lr = 1e-3) with cross entropy loss

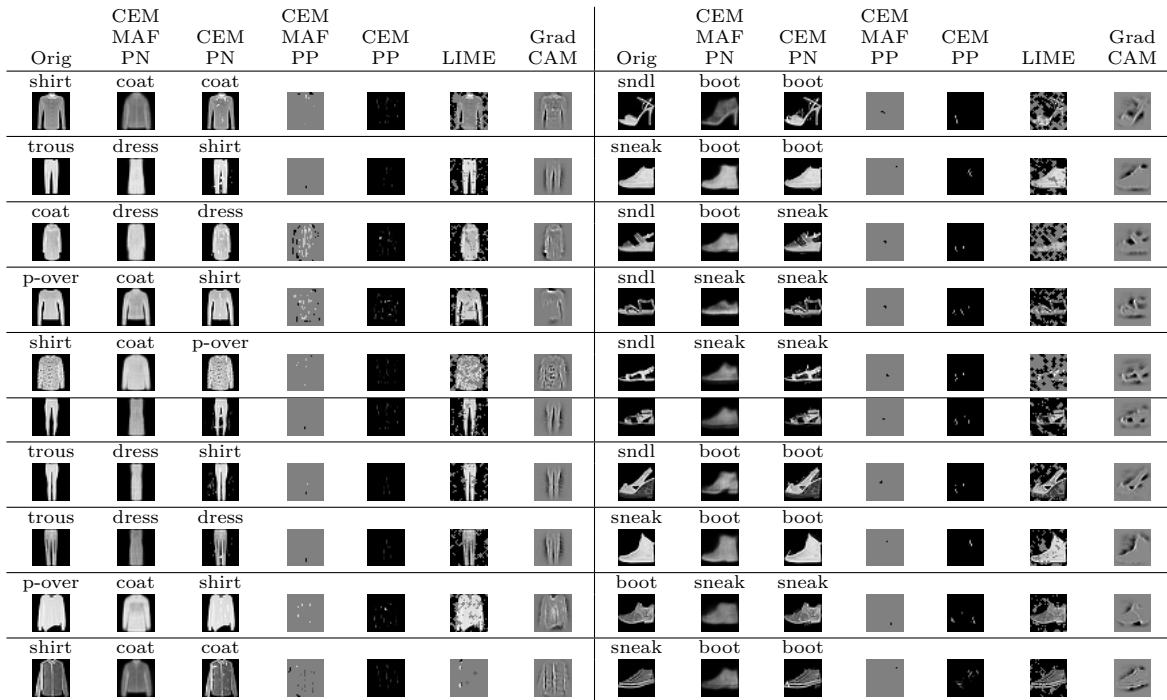
Table 6: Quantitative comparison of CEM-MAF, LIME, and Grad-CAM on the Fashion MNIST datasets.

<b>Dataset</b>	<b>Method</b>	<b># PP Feat</b>	<b>PP Acc</b>	<b>PP Corr</b>
Fashion MNIST	CEM-MAF	62.7	100	-.766
	LIME	226.2	90	-.787
Clothes	Grad-CAM	344.0	100	.077
Fashion MNIST	CEM-MAF	15.7	100	-.947
	LIME	194.1	100	-.800
Shoes	Grad-CAM	202.3	100	-.500

features, but here LIME does better at selecting useful features (PP Correlation close to -1 for clothes). Additionally, LIME and Grad-CAM both have high PP Accuracy, but that is due to selecting many more features.

Rather, contrastive explanations (relative to other items) about what is absent leads to the most intuitive explanations for these images. That same shirt is a shirt because it does not have wide sleeves and is not wide around the waist. In the second row of Figure 7 (b) are classified as trousers because the connection between the legs is absent, and in the fifth row, the item is classified as a shirt because a solid color (more likely on a coat) is absent (i.e., there is a pattern). In the first row of Figure 7 (b), the item is a sandal because it is not thick (i.e., it is an open shoe), while the second item is a sneaker (rather than an ankleboot) because it is missing a heel. The other rows in Figure 7 demonstrate similar explanations.





(a) Fashion-MNIST clothes dataset

(b) Fashion-MNIST shoes dataset

Figure 7: CEM-MAF examples on Fashion-MNIST (a) clothes and (b) shoes dataset. CEM-MAF PN/PP are compared with CEM PN/PP from [6], LIME, and Grad-CAM. Note the abbreviations: p-over for pullover, trous for trousers, boot for ankleboot, and sneak for sneakers.

## 5 User Study

Age demographics for the user study can be found in Table 7. Figure 8 shows a screenshot of a single trial in the user study. As discussed in the paper, a user is first shown an original image with prediction. Then the user is presented with an explanation, CEM-MAF in this instance, and asked to assess the usefulness of the image. A second explanation then pops up, Grad-CAM in this instance, and the user is asked to assess the additional value of this second explanation, after which the user would click on “Next” button and move to the next trial.

Table 7: Age of participants in user study.

Age	Count
18-29	36
30-39	81
40-49	49
50-59	17
Over 60	15

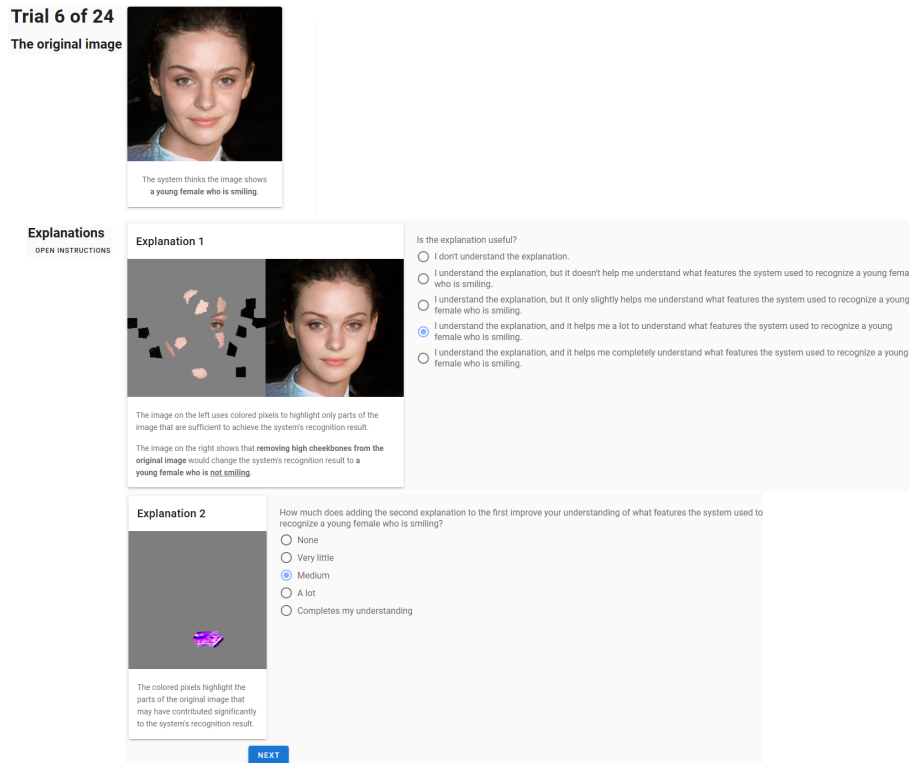


Figure 8: User study survey screen shot. This is an example of a trial where the first explanation offered as CEM-MAF and the user assesses its usefulness, after which the user is presented with another explanation, Grad-CAM in this instance, and asked to assess the additional value of the second explanation.